Visualisation of the actin cytoskeleton by cryo-electron microscopy

Guenter P. Resch[1], Kenneth N. Goldie[2], Angelika Krebs[2], Andreas Hoenger[2] and J. Victor Small[1,*]

[1]Institute of Molecular Biology, Department Cell Biology, Billrothstrasse 11, A-5020 Salzburg, Austria
[2]European Molecular Biology Laboratory, Structure Programme, Meyerhofstrasse 1, D-69117 Heidelberg, Germany
*Author for correspondence (e-mail: jvsmall@imb.oeaw.ac.at)

Accepted 12 February 2002
Journal of Cell Science 115, 1877-1882 (2002)

Summary

An understanding of the mechanisms driving cell motility requires clarification of the structural organisation of actin filament arrays in the regions of cell protrusion termed lamellipodia. Currently, there is a lack of consensus on lamellipodia organisation stemming from the application of alternative procedures for ultrastructural visualisation of cytoskeleton networks. In this study, we show that cryo-electron microscopy of extracted cytoskeletons embedded in a thin layer of vitreous ice can reveal the organisation of cytoskeletal elements at high resolution. Since this method involves no dehydration, drying and contrasting steps that can potentially introduce subtle distortions of filament order and interactions, its application opens the way to resolving the controversial details of lamellipodia architecture.

Key words: Actin, Cytoskeleton, Lamellipodium, Motility, Cryo-electron microscopy

Introduction

The first sign of movement of a eukaryotic cell is the protrusion of a thin sheet of cytoplasm from its periphery, around 0.2 μm thick, called a lamellipodium (Abercrombie et al., 1971). Lamellipodia can extend up to several micrometers and their protrusion is driven by the polymerisation of actin filaments, which form their structural core (reviewed by Small, 1988; Pantaloni et al., 2001). How actin filaments are engaged in protrusive events is a long standing question that now receives keen attention with the recent discovery of several of the molecular players involved in lamellipodia formation (Machesky and Insall, 1998; Higgs and Pollard, 1999; Pantaloni et al., 2001). Among these players is the ubiquitous Arp2/3 complex, which is uniformly distributed in lamellipodia (Welch et al., 1997) and whose role in protrusion appears essential (Machesky and Insall, 1998).

When actin is polymerised in vitro, together with the Arp2/3 complex, branched arrays can be observed (Blanchoin et al., 2000) that arise from the integration of the Arp2/3 complex into the branch points (Pantaloni et al., 2001; Volkmann et al., 2001). The relevance of such actin branching to the in vivo situation was suggested by studies that applied a modified method of critical point drying for electron microscopy and immuno-electron microscopy to the actin cytoskeleton (Svitkina et al., 1995; Svitkina and Borisy, 1998; Svitkina and Borisy, 1999). In captivating images of lamellipodia from keratocytes and fibroblasts, branched arrays of actin filaments were identified and the Arp2/3 complex was localised at the putative branch sites. According to these findings and those of the in vitro studies (Mullins et al., 1998), Svitkina and Borisy have proposed 'treadmilling of a branched actin array' to explain lamellipodia protrusion (Svitkina and Borisy, 1999). However, the credibility of this model rests on the assumption that the method adopted for electron microscopy delivers a faithful image of actin filament networks in situ.

We have previously highlighted the particular susceptibility of actin filament networks, as observed in lamellipodia, to distortion during various preparative steps commonly used in electron microscopy (Maupin-Szamier and Pollard, 1978; Small, 1981; Small, 1985; Small, 1988; Small et al., 1999). And since obvious filament branching was not previously observed in lamellipodia prepared by negative staining methods (reviewed by Small et al., 1999), the possibility of artefacts by one or another method must be seriously considered. In this connection, we have more recently shown (Resch et al., 2002) that the branching of actin filaments is induced in concentrated suspensions of pure F-actin by the same critical point procedure as used previously on cytoskeletons (Svitkina and Borisy, 1999). To resolve current discrepancies over lamellipodia organisation, including the differences observed in quick-freeze deep-etch preparations (Heuser and Kirschner, 1980; Hartwig and Shevlin, 1986; Flanagan et al., 2001), alternative methods must be adopted for structure analysis.

A method that obviates steps that could introduce artefacts is cryo-electron microscopy (see also Discussion). To date, this method has been applied mainly to viruses (Böttcher et al., 1997; Baker et al., 1999), membrane proteins (Henderson et al., 1990; Miyazawa et al., 1999), macromolecular structures (Frank et al., 1995; Schatz et al., 1995) and helical structures (Amos, 2000; Beuron and Hoenger, 2001); examples of larger structures in vitreous ice are limited (reviewed by McIntosh, 2001). In the present study we demonstrate the feasibility of applying cryo-electron microscopy to cytoskeletons and in particular to the analysis of lamellipodia architecture. This first report opens the way to resolving current discrepancies over

filament-filament interactions in this vital organelle of cell motility.

Materials and Methods

Holey carbon support films

As a growth substrate for cells we used holey support films. The method for making holey formvar films that gave the most suitable number and size distribution of holes (see Results) was derived from that described in Hodgkinson and Steffen (Hodgkinson and Steffen, 2001). After addition of five droplets of 50% glycerol to 50 ml of a 0.5% solution of formvar in chloroform, the solution was shaken vigorously for 1 minute and the resulting turbid sol sonified for 3 minutes with a microprobe sonicator at 400 W. Immediately after sonication, a cleaned slide was dipped into this solution and the dried film floated onto a water surface. 200 mesh Ni grids or H2 Ni finder grids (Graticules Ltd., Tonbridge, UK) were placed on the film, which was recovered by a piece of filter paper. Following drying, the formvar/grids/filter paper assembly was placed onto a bed of filter paper saturated with methanol for 10 minutes to perforate pseudoholes. The dried assembly was transferred to an Edwards 306 high vacuum evaporator and coated with a heavy dark grey layer of carbon from a pointed source. The residual formvar film was subsequently dissolved by a 2 hour incubation on a bed of filter paper saturated with 1,2-dichlorethane. After final drying, the grids were stored individually in grid boxes.

Video microscopy

For live imaging of cells moving over holey films, we used GFP-actin or GFP-VASP transfected stable B16F1 clones (Ballestrem et al., 1998; Rottner et al., 1999). The holey carbon support films were UV sterilised, coated on the filmed side with laminin (Sigma, Vienna; floating on a drop of 25 μg/ml in PBS for 1 hour) for improved spreading of the cells, rinsed twice with PBS (150 mM NaCl, 3 mM NaH_2PO_4, 8 mM Na_2HPO_4, pH 7.4) and immediately transferred to dishes with cell culture medium (for details, see Hahne et al., 2001). B16 cells were plated on these films and allowed to spread overnight.

Individual grids were mounted upside-down in microscopy medium (Ham's F12 medium, Sigma-Aldrich, Austria, with 10% FCS) with aluminum fluoride (50 μM $AlCl_3$, 30 mM NaF final concentration) in a 37°C heat controlled chamber; the mount consisted of two pairs of sandwiched grids as lateral clips that were fixed by grease to a coverslip and that held the grid above the coverslip surface, with the cells down. Video microscopy was carried out as described (Hahne et al., 2001) using a 63× oil immersion lens and with acquisition of fluorescence and phase contrast image pairs at intervals of 25 seconds. The individual contrast enhanced frames from the fluorescence channel were aligned with the help of the hole pattern seen in phase contrast and merged with a phase contrast image previously enhanced with an edge filter.

Preparation of extracted cytoskeletons

B16F1wt mouse melanoma cells (American Type Culture Collection) were plated on the holey carbon films and allowed to spread overnight as described above. The formation of extensive lamellipodia was induced by the application of aluminum fluoride 20-30 minutes prior to fixation. Cells were washed briefly with prewarmed PBS and extracted with one of two protocols previously used as a first step for subsequent negative staining (Small and Sechi, 1998) or critical point drying (Svitkina and Borisy, 1999). (1) Extraction/fixation in 0.25% Triton X-100 and 0.5% EM grade glutaraldehyde (GA) in cytoskeleton buffer (CB; 150 mM NaCl, 5 mM EGTA, 5 mM $MgCl_2$, 5 mM glucose, 10 mM MES, pH 6.1) for 1-5 minutes; or (2) extraction in 1% Triton X-100 in PEM (1 mM $MgCl_2$, 1 mM EGTA, 100 mM PIPES pH 6.9) with added 4% polyethylene glycol (PEG), molecular mass 20 kDa. Both extraction solutions included Alexa Fluor 488 phalloidin (Molecular Probes) at a dilution of 1:300 (22 nM) as an actin filament label for correlative light microscopy. In both cases the cytoskeletons were post-fixed with 1% GA in CB for 20-60 minutes with the same amount of fluorescently labelled phalloidin added.

Some samples on finder grids were transferred to a chamber filled with CB mounted on an inverted fluorescence microscope for 'mapping' of cells prior to electron microscopy. Images were taken in both phase contrast and GFP fluorescence channels and merged after edge filtering of the phase contrast image. Immediately before freezing, the samples were washed with CB briefly, mounted in the freeze plunger, blotted on the front (cell) side and plunged into liquid ethane. The grids were stored in water-free liquid nitrogen until inspection.

Electron microscopy

Frozen hydrated samples were examined with a Philips CM 200 FEG at 200 kV in TEM low-dose bright-field mode. A GATAN 626 cryostage cooled to approximately 90 K by liquid nitrogen was used. An optimal balance between contrast and resolution was given at a defocus of –2.5 μm, which is within the range applied by Lepault et

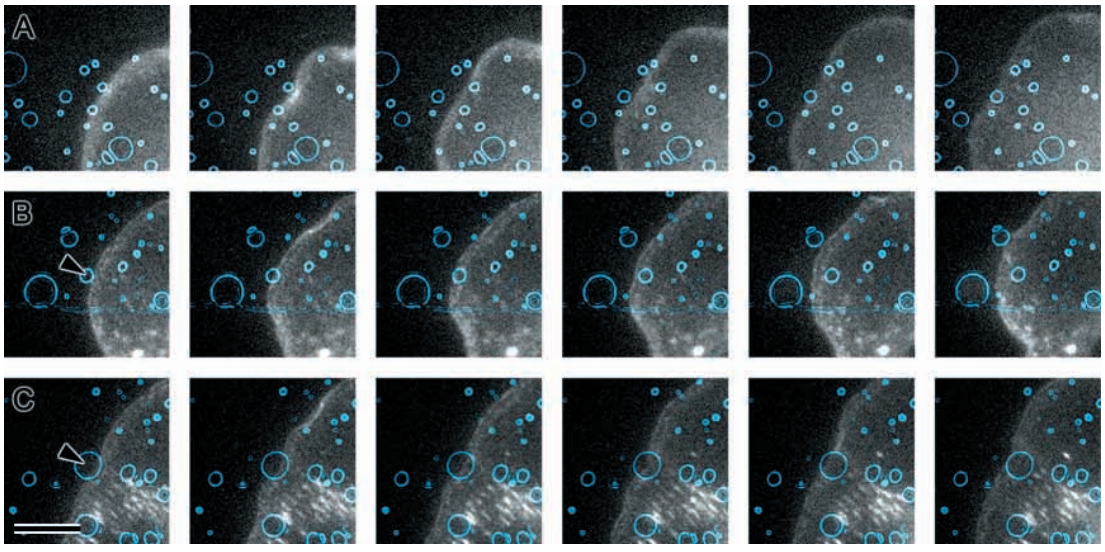

Fig. 1. Time lapse series of lamellipodia crossing the holes of a perforated film. (A) GFP-actin-transfected B16F1 melanoma cell; the holes in the lamellipodium region in this sequence are 1-2 μm in diameter. (B,C) GFP-VASP-expressing B16 cells. The central 2 μm (B) and 4 μm (C) holes are indicated by arrowheads; the 4 μm hole causes a temporary delay in local protrusion. Each sequence covers approximately 10 minutes. Bar, 10 μm.

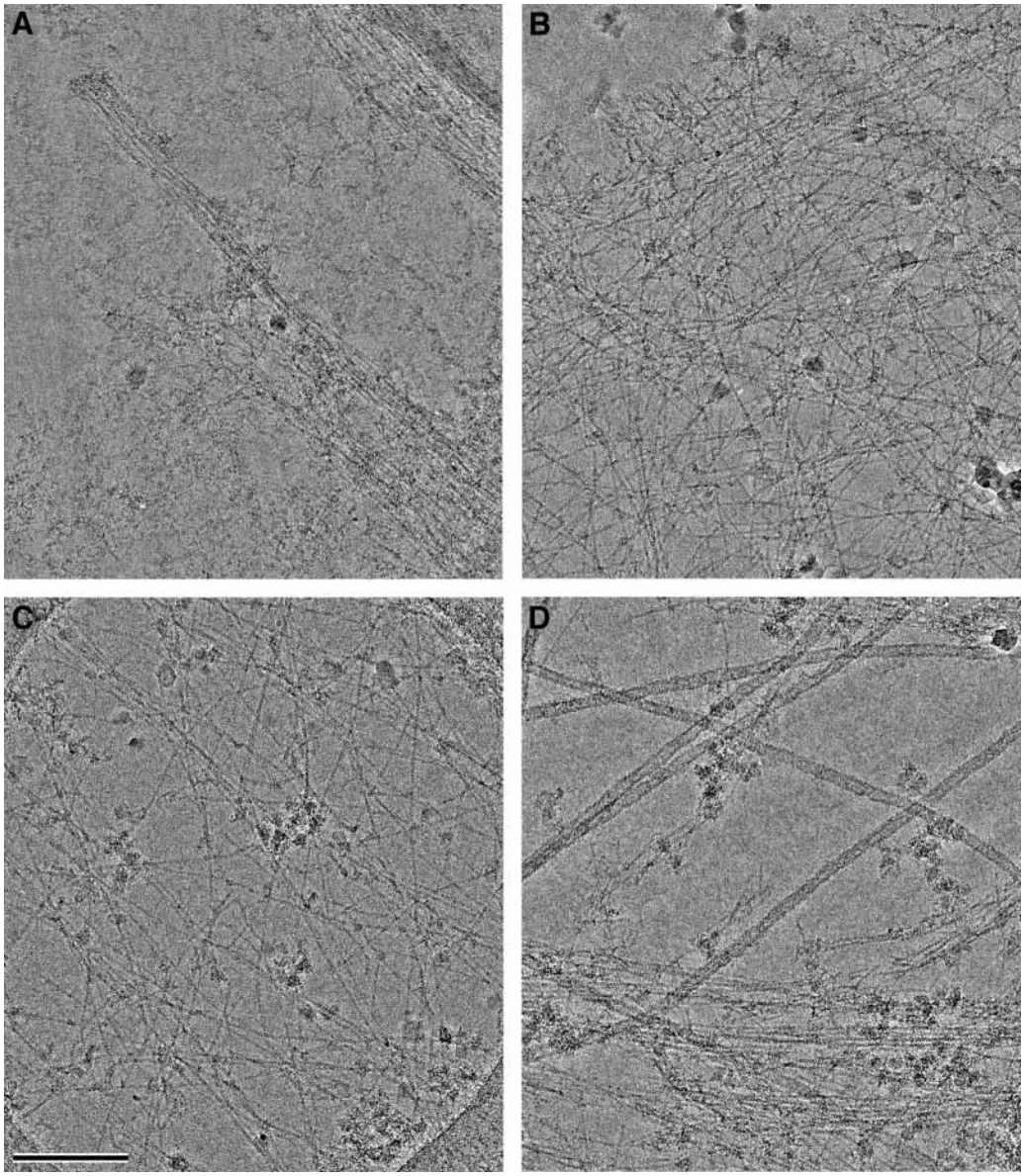

Fig. 2. Images of the actin cytoskeleton in frozen hydrated samples; the cytoskeletons were produced by 1 minute extraction in the Triton/GA mixture. (A) A filopodium protruding at the cell's edge; in the top right corner, another thick filopodium is seen. (B) A lamellipodium showing a relatively sparse network, together with filaments arranged parallel to the edge, probably corresponding to a non-protruding region (see text). (C) Sparse actin networks found in regions deeper inside the lamella; the globular structures of approximately 20×30 nm seen frequently are interpreted as ribosomes. (D) Another lamella region showing F-actin, microtubules and ribosomes. Bar, 200 nm.

al. on synthetic actin filaments (Lepault et al., 1994); typically, holes of a diameter between around 1.5 and 3.0 μm were used for imaging. Since the cell's outline was almost impossible to localise at low magnification, images were taken either in proximity of the clearly visible perinuclear area or according to coordinates established by mapping in the fluorescence microscope.

Electron micrographs were acquired on 3.25×4 inch Kodak Electron SO-163 plate film; negatives were digitised with a Zeiss SCAI or with an Umax Astra 2400S scanner, both using a resolution of 21 μm. For improvement of image quality, a high pass filter (Adobe PhotoShop 5.5) was applied to all images, together with an appropriate adjustment of contrast.

Results

Holey films as a cell substrate

In frozen hydrated samples, contrast is obtained by defocusing only and, in order to reduce background, suspensions of molecules and filaments are commonly viewed in film-free areas of highly perforated support films. For cells, this option is not possible; however, the use of holey carbon films with a substantially lower hole/film ratio as a growth substrate offered a solution. The problem here was to create a range of hole sizes at a density distribution that still allowed normal cell spreading and movement (see Materials and Methods). Motility on the films was analysed by video microscopy of B16 melanoma cells (Fig. 1), which express either GFP-actin (Ballestrem et al., 1998) or GFP-VASP (Rottner et al., 1999). GFP-VASP marks the front edge of the lamellipodium and is therefore a particularly good marker for shape perturbations. As shown in Fig. 1A,B, the movement of lamellipodia was unperturbed when crossing holes of 2-3 μm in diameter. Holes of 4 μm (Fig. 1C) were also readily traversed but, in this case, advance of the lamellipodia lateral to the hole was required to support translocation over the hole. Therefore, holes in the range of 2-3 μm diameter were targeted in the present analysis.

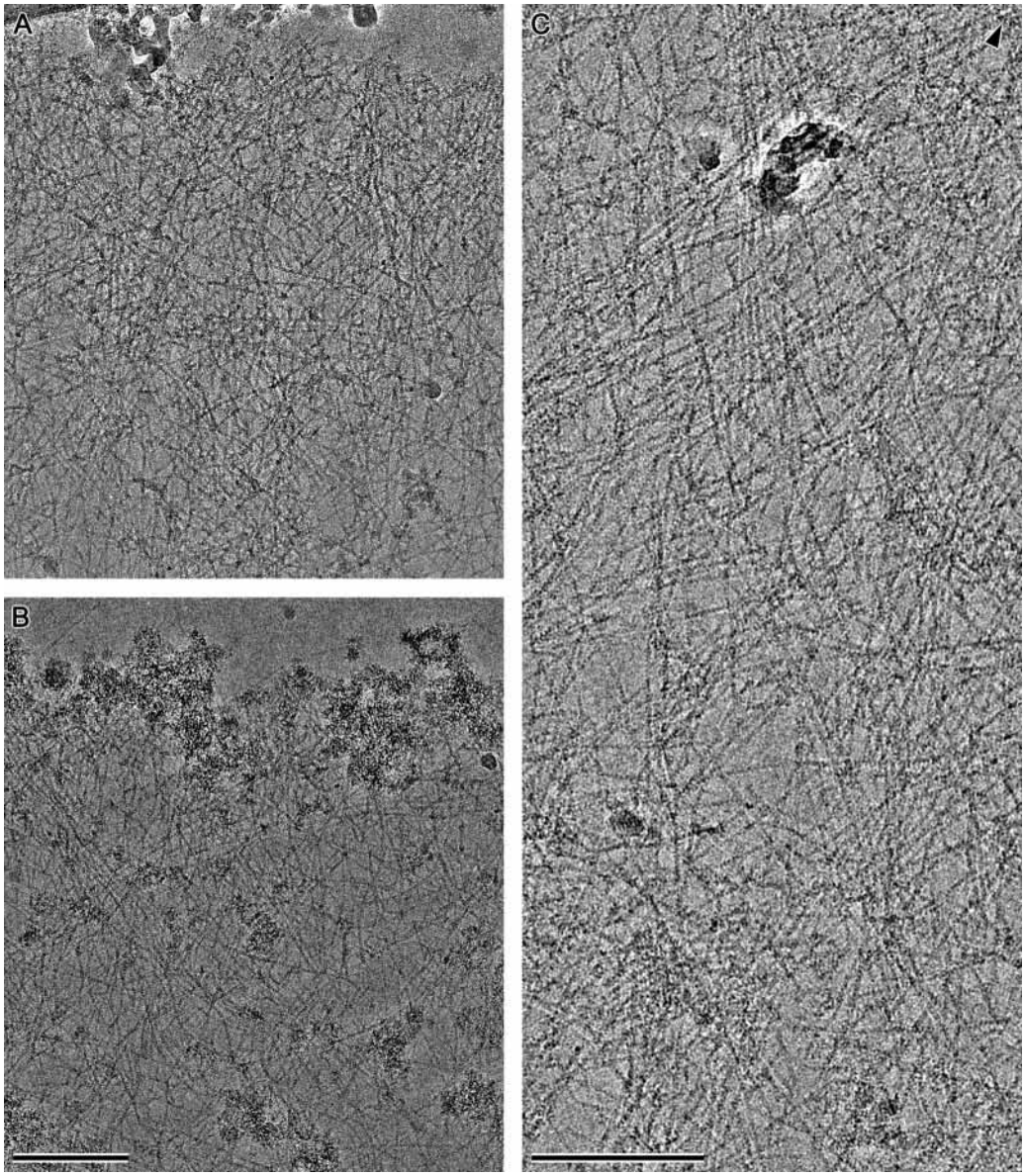

Fig. 3. Lamellipodia regions in mouse melanoma cells, extracted either with the Triton/glutaraldehyde mixture (1 minute; A,C) or with Triton/PEG (B). The grainy aggregates seen in (B) are typical of this extraction procedure. In C, the very front of the lamellipodium is 0.2 μm from the top edge, in the direction indicated by the arrowhead. Bar, 200 nm (A,B); 200 nm (C).

Cryo-EM yields high resolution images of the cytoskeleton

In the cryo-electron microscope, the outline of cells was not obvious and only correlative light and electron microscopy or changes in ice thickness allowed their approximate location. By selecting holes in such regions where the ice layer was sufficiently thin, clear images of actin filament arrays and microtubules were obtained (Figs 2, 3). Fig. 2A and B correspond to peripheral regions showing a filopodium (A) and a lamellipodium (B), while Fig. 2C and D show interior lamella regions. The high incidence of filaments running closely parallel to the cell front in Fig. 2B suggests that this region was more or less stationary at the time of fixation (Rinnerthaler et al., 1991).

Further images of lamellipodia are shown in Fig. 3 and exhibit a filament organisation more typical of protruding regions of B16 melanoma cells, as judged by the use of negative staining on cells fixed during active protrusion (Rottner et al., 1999) (J.V.S., unpublished). This figure shows lamellipodia from cytoskeletons extracted by the two alternative procedures described in Materials and Methods and corresponding to an initial Triton/GA treatment in Fig. 3A,C and a Triton/PEG extraction in Fig. 3B. For the PEG method (Svitkina and Borisy, 1999), we consistently observed dense aggregates of material that were not removed by relatively extensive washing in buffer and that were concentrated, in particular, at the lamellipodium tip (presumably PEG). We observed similar aggregates in negatively stained samples extracted with the same protocol (J.V.S., unpublished). Nevertheless, the contrast and organisation of filaments in lamellipodia was comparable for both extraction methods. Fig. 3C shows a medial region of a lamellipodium; the clarity of the filament organisation is surprisingly close to that observed by the negative staining procedure (Small, 1988; Small et al., 1999). The actin filament substructure is clearly resolved in these images.

Tracing of filaments in single cryo-EM images to estimate the mean length is limited by several factors including the

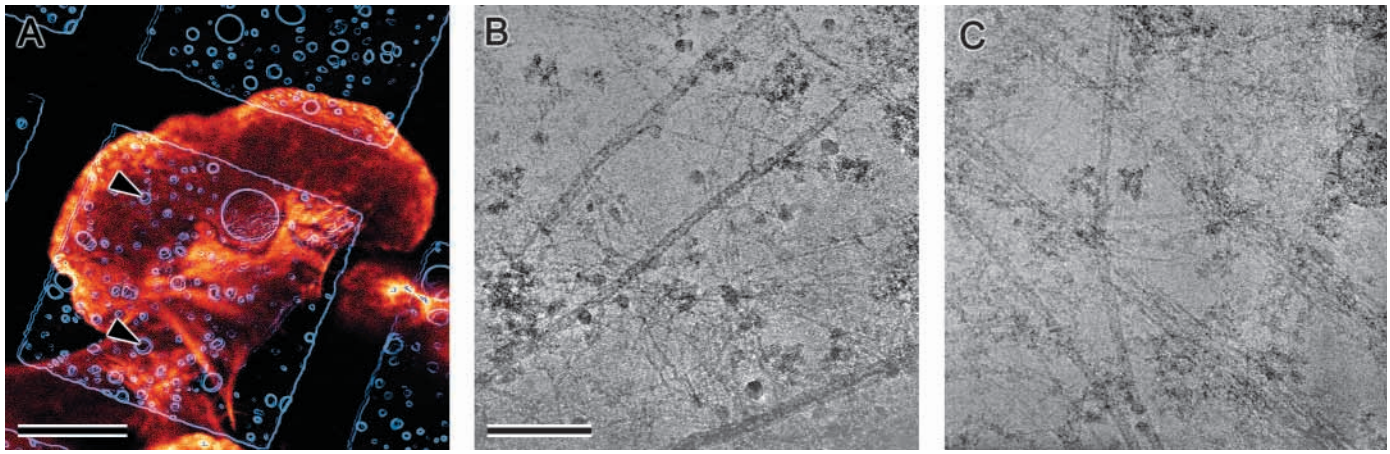

Fig. 4. Correlation of light microscope and cryo-EM images. (A) Phalloidin-actin stain merged with a filtered phase contrast image of the holey film. (B,C) Details from the labelled holes in (A), showing actin filaments, microtubules and ribosomes. Bar , 20 μm (A); 200 nm (B,C).

dimension of the hole, the high filament density and low filament contrast. Nevertheless, filaments up to 0.5 μm in a 1 μm region at the front of protruding edges could be observed. In an initial analysis, we manually traced filaments and scored the length distribution. These measurements showed that approximately 30-35% of the total filament length was contributed by filaments longer than 200 nm. Further analysis using other processing procedures or stereo imaging will be required to obtain a more reliable estimate.

In this first report, we have not made direct correlations of the same regions in cells by video microscopy and cryo-EM. However, the feasibility of the approach is indicated in Fig. 4. Thus, the combined use of finder grids and the irregular hole pattern of the films allows the location of specific areas in the cryo-EM with cells labelled with a fluorescent marker. The globular structures in Fig. 4B,C are interpreted as ribosomes retained in the cytoskeleton.

Discussion

All studies of cytoskeletal architecture of whole mount cell preparations have so far relied on protocols involving detergents to remove the cell membrane, either before or during fixation. Both our own results (data not shown) with unextracted frozen hydrated cells as well as the data from previous studies (O'Toole et al., 1993) show the need for extraction in order to visualise the actin system with full clarity. This represents a limitation that has yet to be properly controlled with regard to the relative loss of lamellipodia components. Nevertheless, such protocols applied to living cells under direct observation in the light microscope have been shown to preserve cell morphology (Rinnerthaler et al., 1988; Rinnerthaler et al., 1991; Svitkina and Borisy, 1999; Small et al., 1999) and to retain lamellipodia-associated proteins (Small et al., 1982; Hartwig and Shevlin, 1986; Svitkina and Borisy, 1999; Rottner et al., 1999; Flanagan et al., 2001), although the amounts retained have yet to be quantitated.

Following extraction and fixation, the different EM procedures that have been applied require one or more preparative steps. The critical point drying procedure entails the most steps, including post-fixations with tannic acid and uranyl acetate, dehydration in ethanol, critical point drying and shadowing (Svitkina and Borisy, 1999). By contrast, negative staining is a one step drying and contrasting procedure. Quick freeze deep etching and cryo-EM share a similar freezing step, following blotting of excess liquid, but the deep etch method requires further steps of ice sublimation under vacuum and contrasting by shadowing (Heuser and Kirschner, 1980). An important difference between the two freezing methods, apart from the sublimation step, lies in the possibility of cryo-EM to directly assess the local quality of freezing, namely whether the ice was vitreous or not. With the reservations already noted on the extraction protocol, the cryo-EM method therefore offers the least possibility of creating artefacts in filament organisation. The disadvantage of the method lies in the need to restrict viewing through holes in the substrate, in addition to the expensive instrumentation and demanding imaging protocols.

The validity of analysing lamellipodia structure over holes is indicated by the known characteristics of lamellipodia protrusion. As others have shown, the extension of lamellipodia can readily occur above a substrate (Izzard and Lochner, 1980). In the case of B16 melanoma cells, advancing lamellipodia are typically 2-5 μm across and protrusion on laminin is supported by adhesion at the lamellipodium base by focal complexes (Rottner et al., 1999). It can therefore be assumed that lamellipodia extending over holes of 2-3 μm in diameter have a structure typical of neighbouring regions extending over substrate. The present findings thus pave the way for a critical analysis of lamellipodium architecture. By pursuing this approach in combination with 3D imaging (Grimm et al., 1997) it should be possible to reach a consensus on the extent of actin filament branching in lamellipodia. Likewise, future prospects include a more precise localisation of the many lamellipodia-associated proteins (reviewed by Small et al., 2002) to shed further light on the structure-function relationships underlying actin-based protrusion in cell motility.

The authors thank Raphaela Rid, Irina Kaverina (Institute of Molecular Biology, Salzburg) as well as Timo Zimmermann (ALMF EMBL Heidelberg) for their help with light- and video microscopy.

References

Abercrombie, M., Heaysman, J. E. and Pegrum, S. M. (1971). The locomotion of fibroblasts in culture. IV. Electron microscopy of the leading lamella. *Exp. Cell. Res.* **67**, 359-367.

Amos, L. A. (2000). Focusing-in on microtubules. *Curr. Opin. Struct. Biol.* **10**, 236-241.

Baker, T. S., Olson, N. H. and Fuller, S. D. (1999). Adding the third dimension to virus life cycles: three-dimensional reconstruction of icosahedral viruses from cryo-electron micrographs. *Microbiol. Mol. Biol. Rev.* **63**, 862-922.

Ballestrem, C., Wehrle-Haller, B. and Imhof, B. A. (1998). Actin dynamics in living mammalian cells. *J. Cell Sci.* **111**, 1649-1658.

Beuron, F. and Hoenger, A. (2001). Structural analysis of the microtubule-kinesin complex by cryo-electron microscopy. *Methods Mol. Biol.* **164**, 235-254.

Blanchoin, L., Amann, K. J., Higgs, H. N., Marchand, J. B., Kaiser, D. A. and Pollard, T. D. (2000). Direct observation of dendritic actin filament networks nucleated by Arp2/3 complex and WASP/Scar proteins. *Nature* **404**, 1007-1011.

Böttcher, B., Wynne, S. A. and Crowther, R. A. (1997). Determination of the fold of the core protein of hepatitis B virus by electron cryomicroscopy. *Nature* **386**, 88-91.

Flanagan, L. A., Chou, J., Falet, H., Neujahr, R., Hartwig, J. H. and Stossel, T. P. (2001). Filamin A, the Arp2/3 complex, and the morphology and function of cortical actin filaments in human melanoma cells. *J. Cell Biol.* **155**, 511-518.

Frank, J., Zhu, J., Penczek, P., Li, Y., Srivastava, S., Verschoor, A., Radermacher, M., Grassucci, R., Lata, R. K. and Agrawal, R. K. (1995). A model of protein synthesis based on cryo-electron microscopy of the E. coli ribosome. *Nature* **376**, 441-444.

Grimm, R., Barmann, M., Hackl, W., Typke, D., Sackmann, E. and Baumeister, W. (1997). Energy filtered electron tomography of ice-embedded actin and vesicles. *Biophys. J.* **72**, 482-489.

Hahne, P., Sechi, A., Benesch, S. and Small, J. V. (2001). Scar/WAVE is localised at the tips of protruding lamellipodia in living cells. *FEBS Lett.* **492**, 215-220.

Hartwig, J. H. and Shevlin, P. (1986). The architecture of actin filaments and the ultrastructural location of actin-binding protein in the periphery of lung macrophages. *J. Cell Biol.* **103**, 1007-1020.

Henderson, R., Baldwin, J. M., Ceska, T. A., Zemlin, F., Beckmann, E. and Downing, K. H. (1990). Model for the structure of bacteriorhodopsin based on high-resolution electron cryo-microscopy. *J. Mol. Biol.* **213**, 899-929.

Heuser, J. E. and Kirschner, M. W. (1980). Filament organization revealed in platinum replicas of freeze-dried cytoskeletons. *J. Cell Biol.* **86**, 212-234.

Higgs, H. N. and Pollard, T. D. (1999). Regulation of actin polymerization by Arp2/3 complex and WASp/Scar proteins. *J. Biol. Chem.* **274**, 32531-32534.

Hodgkinson, J. L. and Steffen, W. (2001). Direct labeling of components in protein complexes by immuno-electron microscopy. *Methods Mol. Biol.* **161**, 133-139.

Izzard, C. S. and Lochner, L. R. (1980). Formation of cell-to-substrate contacts during fibroblast motility: an interference-reflexion study. *J. Cell Sci.* **42**, 81-116.

Lepault, J., Ranck, J.-L., Erk, I. and Carlier, M. F. (1994). Small angle X-ray scattering and electron cryomicroscopy study of actin filaments: role of the bound nucleotide in the structure of F-actin. *J. Struct. Biol.* **112**, 79-91.

Machesky, L. M. and Insall, R. H. (1998). Scar1 and the related Wiskott-Aldrich syndrome protein, WASP, regulate the actin cytoskeleton through the Arp2/3 complex. *Curr. Biol.* **8**, 1347-1356.

Maupin-Szamier, P. and Pollard, T. D. (1978). Actin filament destruction by osmium tetroxide. *J. Cell Biol.* **77**, 837-852.

McIntosh, J. R. (2001). Electron microscopy of cells: a new beginning for a new century. *J. Cell Biol.* **153**, F25-F32.

Miyazawa, A., Fujiyoshi, Y., Stowell, M. and Unwin, N. (1999). Nicotinic acetylcholine receptor at 4.6 A resolution: transverse tunnels in the channel wall. *J. Mol. Biol.* **288**, 765-786.

Mullins, R. D., Heuser, J. A. and Pollard, T. D. (1998). The interaction of Arp2/3 complex with actin: nucleation, high affinity pointed end capping, and formation of branching networks of filaments. *Proc. Natl. Acad. Sci. USA* **95**, 6181-6186.

O'Toole, E., Wray, G., Kremer, J. and McIntosh, J. R. (1993). High voltage cryomicroscopy of human blood platelets. *J. Struct. Biol.* **110**, 55-66.

Pantaloni, D., Le Clainche, C. and Carlier, M. F. (2001). Mechanism of actin-based motility. *Science* **292**, 1502-1506.

Resch, G. P., Goldie, K. N., Hoenger, A. and Small, J. V. (2002). Pure F-actin networks are distorted and branched by steps in the critical point drying method. *J. Struct. Biol.* (in press).

Rinnerthaler, G., Geiger, B. and Small, J. V. (1988). Contact formation during fibroblast locomotion: involvement of membrane ruffles and microtubules. *J. Cell Biol.* **106**, 747-760.

Rinnerthaler, G., Herzog, M., Klappacher, M., Kunka, H. and Small, J. V. (1991). Leading edge movement and ultrastructure in mouse macrophages. *J. Struct. Biol.* **106**, 1-16.

Rottner, K., Behrendt, B., Small, J. V. and Wehland, J. (1999). VASP dynamics during lamellipodia protrusion. *Nat. Cell Biol.* **1**, 321-322.

Schatz, M., Orlova, E. V., Dube, P., Jager, J. and van Heel, M. (1995). Structure of Lumbricus terrestris hemoglobin at 30 Å resolution determined using angular reconstitution. *J. Struct. Biol.* **114**, 28-40.

Small, J. V. (1981). Organization of actin in the leading edge of cultured cells: influence of osmium tetroxide and dehydration on the ultrastructure of actin meshworks. *J. Cell Biol.* **91**, 695-705.

Small, J. V. (1985). Factors affecting the integrity of actin meshworks in cultured cells. In *Cell Motility: Mechanism and Regulation* (ed. H. Ishikawa, S. Hatano and H. Sato), pp. 493-506. Tokyo: University of Tokyo Press.

Small, J. V. (1988). The actin cytoskeleton. *Electron Microsc. Rev.* **1**, 155-174.

Small, J. V. and Sechi, A. (1998). Whole-mount electron microscopy of the cytoskeleton: negative staining methods. In *Cell Biology: a Laboratory Handbook*, 2nd edn, Vol. 3 (ed. J. E. Celis), pp. 285-291. San Diego: Academic Press.

Small, J. V., Rinnerthaler, G. and Hinssen, H. (1982). Organization of actin meshworks in cultured cells: the leading edge. *Cold Spring Harb. Symp. Quant. Biol.* **46**, 599-611.

Small, J. V., Rottner, K., Hahne, P. and Anderson, K. I. (1999). Visualising the Actin Cytoskeleton. *Microsc. Res. Tech.* **47**, 3-17.

Small, J. V., Stradal, T., Vignal, E. and Rottner, K. (2002). The lamellipodium: where motility begins. *Trends Cell Biol.* **12**, 112-120.

Svitkina, T. M. and Borisy, G. G. (1998). Correlative light and electron microscopy of the cytoskeleton of cultured cells. *Methods Enzymol.* **298**, 570-592.

Svitkina, T. M. and Borisy, G. G. (1999). Arp2/3 complex and actin depolymerizing factor/cofilin in dendritic organization and treadmilling of actin filament arrays in lamellipodia. *J. Cell Biol.* **145**, 1009-1026.

Svitkina, T. M., Verkhovsky, A. B. and Borisy, G. G. (1995). Improved procedure for electron microscopic visualization of the cytoskeleton of cultured cells. *J. Struct. Biol.* **115**, 290-303.

Volkmann, N., Amann, K. J., Stoilova-McPhie, S., Egile, C., Winter, D. C., Hazelwood, L., Heuser, J. E., Li, R., Pollard, T. D. and Hanein, D. (2001). Structure of Arp2/3 complex in its activated state and in actin filament branch junctions. *Science* **293**, 2456-2459.

Welch, M. D., DePace, A. H., Verma, S., Iwamatsu, A. and Mitchison, T. J. (1997). The human Arp2/3 complex is composed of evolutionarily conserved subunits and is localized to cellular regions of dynamic actin filament assembly. *J. Cell Biol.* **138**, 375-384.